

Cut-set and Stability Constrained Optimal Power Flow for Resilient Operation During Wildfires

Satyaprajna Sahoo, Anamitra Pal
School of Electrical, Computer and Energy Engineering
Arizona State University
Tempe, United States
sssahoo2@asu.edu, anamitra.pal@asu.edu

Abstract—Resilient operation of the power system during ongoing wildfires is challenging because of the uncertain ways in which the fires impact the electric power infrastructure. For example, wildfires near energized power lines cause arc-faults to occur in rapid succession; such frequent faults can trip multiple grid assets due to dynamic instability. Conventional contingency analysis tools are not equipped to handle such phenomena. To address this challenging problem, we propose a novel cut-set and stability-constrained optimal power flow (CSCOPF) that ensures secure, stable, and economic power system operation through an advanced contingency analysis formulation which quickly detects and mitigates both static and dynamic insecurities as wildfires progress through a region. The CSCOPF achieves its objective by integrating a “feasibility test” algorithm that exhaustively desaturates overloaded cut-sets to prevent cascading line outages and a data-driven transient stability analyzer that predicts the correction factors for eliminating generator trips, with the optimal power flow formulation. The results obtained using the IEEE 118-bus system indicate that the proposed approach alleviates vulnerability of the system to active wildfires while simultaneously minimizing operational cost.

Index Terms—Contingency analysis, Cut-set saturation, Optimal power flow, Static security, Transient stability, Wildfire

I. INTRODUCTION

IN recent years, the prevalence of wildfires has surged, posing monumental challenges for electric power utilities. On one side, they have been blamed for starting devastating wildfires, which have even culminated in some utilities declaring bankruptcy [1]. On the other side, they are expected to maintain secure and stable grid operation in presence of active wildfires to support other critical services. The focus of this paper is on the latter, namely, *ensuring resilient power system operation when a progressing wildfire is projected to intersect a power transmission corridor*.

An analysis of major wildfire-induced power system interruptions has identified *cascading outages resulting from overloaded assets, frequent arc-faults, and/or preemptive disconnection of power system equipment* as the primary causes (for the interruptions) [2], [3]. Overloads occur because the heat from the fires affect the power lines in their vicinity resulting in lowering of the conductor’s current carrying capacity [4]. This lowering may then cause bottlenecks to appear in other

parts of the system. The pioneering work on this topic was done by [5]. However, [5] and the papers that cited it, did not consider the impacts of fire-induced faults on dynamic stability of the power system. During the 2016 Blue Cut Fire, as the fire approached a corridor of three 500kV and two 287kV transmission lines, *15 arc-faults occurred in a short period of time* [6]. Other instances of system instabilities caused by fire-induced arc-faults can be found in [3], [7], [8]. Wildfire induced arc-faults are unique as they occur multiple times within a few seconds [9]. Conventional contingency analysis tools that usually deal with *one fault occurring on a line/lines*, are not equipped to handle such phenomena. At the same time, preemptively disconnecting lines in advance and over wide regions to protect them from *future* arc-faults bears a very high social cost. During the 2019 California fires, preemptive actions by the local utility left more than 2.7 million people without electricity [10]. Since areas impacted by wildfires have grown considerably in the last decade, power utilities must operate their systems till the last-minute while also considering static security (to protect against asset overloads) and dynamic stability (to minimize impact of frequent arc-faults) [11].

In this paper, we introduce a novel cut-set and stability-constrained optimal power flow (CSCOPF) to conduct a comprehensive contingency analysis for active wildfire scenarios, and ensure resilient power system operation upon emergence of such scenarios. A cut-set is a set of lines, which if tripped, would create disjoint islands in the network. Therefore, saturated/overloaded cut-sets are the most vulnerable interconnections of the system [12]. For ensuring static security, we leverage the “feasibility test” (FT) algorithm developed in [13] to *exhaustively* protect the system against saturated cut-sets; we also ensure security against $N - 1$ branch overloads. Dynamic stability is ensured through a data-driven transient stability constraint prediction (TSCP) algorithm that estimates the required transient stability correction factor (TSCF) while accounting for load uncertainties. The outcomes of the two algorithms are added as constraints to the optimal power flow (OPF) formulation (see Fig. 1). The OPF, modeled as an optimal redispatch problem, is run iteratively until all violations are addressed. A case-study conducted using the IEEE 118-bus system demonstrates that the proposed approach is able to alleviate cascading outages due to static and dynamic insecurities with minimal increase in operational cost.

This work was supported in part by the National Science Foundation (NSF) grant under Award ECCS-2132904.

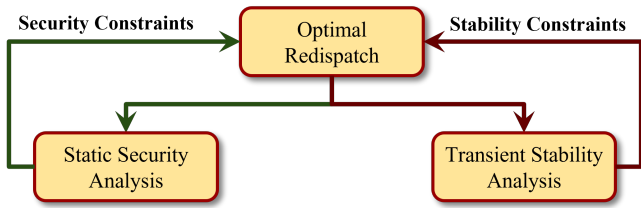


Fig. 1: CSCOPF overview

II. PROBLEM SCOPE AND SOLUTION APPROACH

Wildfires and their interaction with the electric power grid constitutes a multi-faceted problem because of the following reasons: (a) the spatio-temporal process of wildfire spread is based on local climate and geography (topography, vegetation, wind); (b) breakdown mechanisms of the air gap varies with time, location, and wildfire proximity and intensity; (c) outcomes can range from multiple arcing events to a complete line melt-down (permanent outage) [7], [8], [14]. We now specify the problem scope in the context of these facets.

A variety of tools already exist for tracking wildfire spread over different geographical regions (e.g., FlamMap [15]); hence, tracking of wildfires is outside the scope of this paper. Without knowledge of the local environmental conditions around a transmission line when a fire is nearby, it is not possible to determine the air quality and/or the type of event that might occur (frequent multiple arc-faults or permanent outage). In this regard, one strategy could be to assume that all power lines located in an active wildfire area are preemptively de-energized, and then solve an optimal generation redispatch problem in presence of topology changes [16]. However, as explained in [2], such a strategy may not be optimal from a socio-techno-economic perspective.

In this paper, we consider both types of outcomes, namely, multiple arc-faults as well as permanent line outages. To prepare the system for such eventualities, we develop two contingency analysis methods. Although these methods can be used for any extreme event/multi-asset contingency, they are implemented (see Section III-G) considering the unique attributes of wildfires. Lastly, some articles have focused on enhancing the resilience of the power grid against wildfires by system hardening, better asset management, and/or optimally allocating fire-extinguishing resources [4], [17]–[19]. These could be deemed complementary to the scope of this paper.

A. Static Security using Cut-set Analysis

A saturated cut-set is a cut-set whose aggregate power flow exceeds the limits of the constituent lines, as shown below:

$$\sum_{\forall e \in K_{\text{crit}}} f_e > \sum_{\forall e \in K_{\text{crit}}} f_e^{\text{max}} \quad (1)$$

where, f_e denotes the flow in the e^{th} line, f_e^{max} is the maximum flow allowed through that line, and K_{crit} is a saturated cut-set. A transmission corridor of the power system is likely to be a part of one or more cut-sets. The FT algorithm, which takes power injections as its inputs [12], [20], quickly identifies

and alleviates all saturated cut-sets for a given contingency, and is mathematically expressed as,

$$\sum_{\forall e \in K_{\text{crit}}} \Delta f_e \leq -\Delta P_{K_{\text{crit}}} \quad \forall K_{\text{crit}} \in \kappa_{\text{crit}} \quad (2)$$

where, κ_{crit} is the set of all identified cut-sets, and $\Delta P_{K_{\text{crit}}}$ is the identified transfer margin, which is the overall amount of power that must be reduced across the lines in the cut-set to eliminate overloading.

B. Transient Stability using Machine Learning

Transient stability assessment and control evaluates the capability of the power system to maintain synchronism after a large disturbance, such as multiple frequent arc-faults. Different attributes of the system, including system configuration, loading conditions, and fault location, influence the transient stability assessment. In this paper, we focus on the rotor angle stability, which is a key factor in determining transient stability in presence of faults [21]. The rotor angle stability is quantified by the transient stability index (TSI) shown below, where δ_{max} is the maximum difference in the sorted rotor angles of two consecutive machines.

$$\text{TSI} = \frac{360 - \delta_{\text{max}}}{360 + \delta_{\text{max}}} \times 100 \quad (3)$$

The system is stable if $\text{TSI} > 0$, and unstable otherwise. For a contingency that causes TSI to become negative, the total generation is split into two groups, one of which is composed of the critical machines (CM) and the other is composed of the non-critical machines (NM). A machine (i.e., a generator) is deemed critical when it swings away from the rest of the machines. Note that there can be more than one machine that is identified as critical for a given contingency.

Given a contingency, transient stability control can be done by the single machine equivalent (SIME) method [22], which utilizes the equal area criterion (EAC) and multiple time domain simulations (TDSs) per contingency. When an instability occurs in a multi-machine system, the integrated extended equal area criterion (IEEAC) can be employed to correct for the instability. The IEEAC stipulates transferring power (denoted by P_{tr}) from the unstable generators to the stable generators, as shown below [23]:

$$\Delta P_{tr} \geq \left(\frac{-\eta_{us} + \epsilon}{\tau} \right) \cdot \left(\frac{M}{M_{CM}} + \frac{M}{M_{NM}} \right)^{-1} \quad (4)$$

where, M, M_{CM}, M_{NM} are the one machine infinite bus (OMIB) inertia coefficients of the whole system, critical machines (CM), and non-critical machines (NM), respectively, η_{us} and ϵ are the unstable value and desired value of the transient stability margin, and τ is a sensitivity factor. ΔP_{tr} , which is the TSCF, can be used to create the transient stability constraint as shown below:

$$\sum_{\forall i \in CM} \Delta p_i \leq -\Delta P_{tr} \quad (5)$$

Now, the calculation of ΔP_{tr} depends on multiple TDSs for a single contingency, which is computationally expensive to do

in real-time. Furthermore, one must also consider the variability of the loads. To account for both of these factors, we exploit the quasi-linear relationship between the pre-contingency one machine mechanical power and the transient stability margin [23]. Specifically, we posit that *a linear relationship exists between the TSCF and the pre-contingency loading condition*. This is because the pre-contingency mechanical power is linearly related to the loads (l) as $\sum_{i \in G} p_i^m = \sum_{i \in G} p_i^e = \sum_{j \in L} l_j$, where p_i^m and p_i^e denote mechanical and electrical power, respectively, of the i^{th} generator. Consequently, we formulate a linear regression (LR) model with a mean squared error (MSE) loss function that estimates the required TSCF for a given loading condition, as shown below:

$$\Delta \hat{P}_{tr} = \sum_{j \in L} \theta_j l_j + \theta_0 = \Upsilon(l_j) \quad (6)$$

$$J(\theta) = \frac{1}{k} \sum_{i=1}^k (\Delta \hat{P}_{tri} - \Delta P_{tri})^2 \quad (7)$$

where, θ are the weights, $J(\theta)$ is the loss function, and k is the batch size. This LR-based model for estimating the TSCF is referred to as the TSCP algorithm, and is denoted by Υ .

III. CSCOPF FORMULATION AND IMPLEMENTATION

A. Objective and Constraints

CSCOPF is modeled as an optimal redispatch problem to alleviate saturated cut-set, branch overloads, and transient stability violations. The cost (F) of generation dispatch considering a quadratic cost curve, can be expressed as:

$$F_i(p_i) = a_i + b_i p_i + c_i p_i^2 \quad (8)$$

where, a_i, b_i, c_i are the fixed, linear, and quadratic cost coefficients of the i^{th} generator; we also dropped e from the superscript of p_i^e to avoid notational clutter. To derive the cost of generation change, (8) is expressed as

$$\begin{aligned} \Delta F_i(\Delta p_i) &= \{a_i + b_i p_i + c_i p_i^2\} - \{a_i + b_i p_i^0 + c_i (p_i^0)^2\} \\ &= c_i \Delta p_i^2 + (b_i + 2c_i p_i^0) \Delta p_i \end{aligned} \quad (9)$$

where, the superscript 0 in (9) refers to the pre-contingency status. Including load shed (Δl), the overall objective becomes minimizing redispatch as well as load shed, as shown below:

$$\min \sum_{i \in G} (c_i \Delta p_i^2 + d_i \Delta p_i) + \sum_{j \in L} (m_j \Delta l_j) \quad (10)$$

where, $d_i = (b_i + 2c_i p_i^0)$, m_j is the cost of shedding load j , and G and L are the sets of generators and loads in the network. The coefficient m_j is typically chosen to be higher than the generation costs, to disincentivize load shedding.

B. Variable Limit Constraints

The generation rescheduling and load shed are limited by the following equations, where the superscripts max and min refer to the maximum and minimum values of the scripted variables, respectively.

$$p_i^{\min} - p_i^0 \leq \Delta p_i \leq p_i^{\max} - p_i^0 \quad \forall i \in G \quad (11)$$

$$l_j^{\min} - l_j^0 \leq \Delta l_j \leq l_j^{\max} - l_j^0 \quad \forall j \in L \quad (12)$$

C. Branch Flow Constraints

The limits on power flows corresponding to the changes in the generation and loads are given by,

$$\begin{aligned} f_u^{\min} - f_u^0 &\leq \sum_{i \in G} \text{PTDF}_{u,i}^r \Delta p_i - \sum_{j \in L} \text{PTDF}_{u,j}^r \Delta l_j \\ &\leq f_u^{\max} - f_u^0 \quad \forall u \in B \end{aligned} \quad (13)$$

where, $\text{PTDF}_{u,i}^r$ is the power transfer distribution factor of branch u for one unit of power added at bus i and one unit of power withdrawn from reference bus (r), B is the set of all branches, and f_u is the active power flowing in u .

D. Power Balance Constraint

This is ensured by making the aggregate change in generation equal the total load shed, as shown below:

$$\sum_{i \in G} \Delta p_i = \sum_{j \in L} \Delta l_j \quad (14)$$

E. Branch Overload Constraints

The $N - 1$ security criteria must be preserved by the proposed corrective action. This is ensured by using the line outage distribution factor (LODF), as shown below,

$$\begin{aligned} &\sum_{i \in G} (\text{PTDF}_{u,i}^r + \text{LODF}_{u,a} \text{PTDF}_{a,i}^r) \Delta p_i \\ &- \sum_{j \in L} (\text{PTDF}_{u,j}^r + \text{LODF}_{u,a} \text{PTDF}_{a,j}^r) \Delta l_j \\ &\leq f_u^{\max} - f_u^0 + (\text{LODF}_{u,a} f_a^0) \quad \forall u, a \in B, \xi \end{aligned} \quad (15)$$

$$\begin{aligned} &\sum_{i \in G} (\text{PTDF}_{u,i}^r + \text{LODF}_{u,a} \text{PTDF}_{a,i}^r) \Delta p_i \\ &- \sum_{j \in L} (\text{PTDF}_{u,j}^r + \text{LODF}_{u,a} \text{PTDF}_{a,j}^r) \Delta l_j \\ &\geq f_u^{\min} - f_u^0 + (\text{LODF}_{u,a} f_a^0) \quad \forall u, a \in B, \xi \end{aligned} \quad (16)$$

where, $\text{LODF}_{u,k}$ represents the percentage of power in branch u that flows through branch k if there is an outage of branch k , and ξ denotes the contingency set.

F. Cut-set and Transient Stability Constraints

The post contingency cut-set constraint is obtained from the FT, as shown below:

$$\begin{aligned} &\sum_{i \in G} \left(\sum_{\forall u \in K_{\text{crit}}} \text{PTDF}_{u,i}^r \right) \Delta p_i \\ &- \sum_{j \in L} \left(\sum_{\forall u \in K_{\text{crit}}} \text{PTDF}_{u,j}^r \right) \Delta l_j \\ &\leq -\Delta P_{K_{\text{crit}}} \quad \forall K_{\text{crit}} \in \kappa_{\text{crit}} \end{aligned} \quad (17)$$

Similarly the transient stability constraint derived from Υ for a defined contingency is given by,

$$\sum_{i \in \text{CM}} \Delta p_i \leq -\Upsilon(l) \quad (18)$$

Note that the CSCOPF formulation described above is implemented on top of a regular economic dispatch; i.e., it uses the prior economic dispatch solution as a *warm start*.

G. Implementation

The steps that must be followed for implementing the proposed CSCOPF are summarized in Algorithm 1. The implementation occurs over two stages. In the day-ahead stage, contingency analyses is performed for potential wildfire scenarios¹ using SIME to identify instability-inducing contingencies. Identification of the appropriate contingency set is followed by creating a dataset of potential loading conditions obtained from historical load data. The TSCP model, Υ , is then trained to calculate the TSCF for the loading conditions and contingencies in the set. In real-time, the system is run normally until a progressing wildfire is projected to intersect a power transmission corridor. Once this happens, the contingency analysis model is used to generate the cutset and transient stability constraints. Since the CSCOPF constraints are convex², the optimization can quickly generate an optimal redispatch solution that ensures a secure, stable, and economic response to the unfolding wildfire scenario.

Algorithm 1 CSCOPF Implementation

Input: Historical load distributions, contingency information (ξ), and real-time power injections

Output: Generation redispatch (Δp), and load shed (Δl)

Day-ahead Stage:

- 1: Perform random sampling from the historical load distributions to determine potential loading conditions Ξ
- 2: Define empty list of constraints Φ
- 3: **for** loading condition in Ξ **do**
- 4: Perform TDS using ξ
- 5: **if** violations detected **then**
- 6: Generate transient stability constraint using (4)
- 7: Update Φ
- 8: **end if**
- 9: **end for**
- 10: Train Υ using Φ

Real-time Stage:

- 1: Define empty list of constraints Φ
 - 2: Obtain real-time power injection information using [20]
 - 3: Generate cut-set constraint using (17)
 - 4: Generate transient stability constraint using Υ ; see (18)
 - 5: Update Φ with constraints (17) and (18)
 - 6: **while** violations detected **do**
 - 7: CSCOPF: Define objective (10), apply constraints (11)-(16), and add constraints present in Φ
 - 8: Solve CSCOPF to get Δp and Δl
 - 9: Update dispatch and run power flow
 - 10: Run FT and single TDS on updated dispatch
 - 11: **if** violations detected **then**
 - 12: Update Φ and Go to Step 7 of Real-time Stage
 - 13: **end if**
 - 14: **end while**
-

¹The wildfire spread scenarios can be determined using FlamMap [15].

²Equations (11)-(18) are convex as they are a linear function of the decision variables.

IV. RESULTS

The proposed formulation is tested on the well-known IEEE 118-bus system. The system has 54 generators, 186 transmission lines and 99 loads, with a total capacity of 9,966 MW. Simulations and contingency analyses are performed using Siemens' PSSE[®] [24]. The optimization model is solved using Gurobi [25], and the OPF is run using Pandapower [26], an open-source package in Python. All computations are done on a computer with an Intel Core (TM) i7-11800H CPU @2.3GHz with 16GB of RAM and an RTX 3070Ti GPU.

Contingency details for an identified corridor of the 118-bus system that is to be impacted by a progressing wildfire is given in Table I (see first row). When the fire does enter the security buffer [7] of the two lines, a set of five faults is assumed to occur consecutively over a period of three seconds on both the lines, at the end of which the lines suffer a permanent outage. To vary the loads of the 118-bus system, we find typical load variations occurring in the loads of the publicly available 2000-bus Synthetic Texas system [27], and then superimpose those variations on the 118-bus system loads using kernel density estimation. We generate 28,000 samples from the resulting load values to create a dataset for training Υ . This dataset captures the full spectrum of real-time load fluctuations and is representative of the operational variability of the loads for the time horizon considered.

A. Wildfire Contingency Impacts and TSCF Estimation Results

Table I shows the security and stability constraints that are obtained when the contingency mentioned in the first row occurs. Note that the required rescheduling is considerable (second, fifth, and sixth rows). Furthermore, such a large change leads to additional static security violations (overloaded cut-sets), as seen in the third and fourth rows.

TABLE I: Contingency details and alleviation actions

Property	Value
Lines impacted	(23,25),(26,30)
Generation at risk	534 MW
Saturated cut-sets	(26-30,25-27)
Cut-set transfer margin	-187.086 MW
Critical machines (CMs)	25,26
TSCF	-118 MW

Using the contingency analysis and load variation information, the data-driven TSCP algorithm is trained for TSCF prediction in real-time. In Table II, the TSCF estimate obtained using LR is compared with the one obtained using ridge regression, support vector regression (SVR), XGBoost, random forest (RF), elastic net, decision tree (DT), and least absolute shrinkage and selection operator (LASSO). It is observed from the root mean squared error (RMSE) and R^2 scores that LR and ridge regression give the best estimates, while RF, elastic net, DT, and LASSO have comparatively poorer performance.

Now, since the loading conditions are themselves subject to errors, the reliability of the estimation is investigated by calculating the R^2 robustness scores, which is the change in R^2 scores when the error in input is increased. The results

TABLE II: TSCF estimation results using different models

Model	RMSE	R^2	R^2 Robustness	MBD
Linear Regression	0.31	0.98	0.0024	$-0.57e-4$
Ridge Regression	0.31	0.98	0.0027	$-0.57e-4$
SVR	0.42	0.97	0.0028	0.02
XGBoost	0.94	0.85	0.0035	-0.004
Random Forest	1.51	0.61	0.0031	0.005
Elastic Net	2.13	0.22	-0.0003	$-0.93e-4$
Decision Tree	2.33	0.06	-0.0051	0.002
LASSO	2.34	0.06	0.0001	$-0.28e-4$

show that the models are generally resilient to errors in the loads (which was capped at 5%), with LR giving the most consistent outcomes. Finally, Table II shows the mean bias deviation (MBD) results, which represents the average bias in the predictions. It is an indication of whether the trained model is under-estimating or over-estimating, and is calculated using:

$$MBD = \frac{\sum_k (y - \hat{y})}{k} \quad (19)$$

Ideally, MBD should be 0. However, in our case, over-estimation of TSCF is preferred, i.e., a negative value of MBD is better. Again, it can be observed from Table II that LR gives a very small negative value for MBD. These results justify our assertion that a linear model is sufficient for TSCP.

B. CSCOPF Implementation Results

The proposed CSCOPF is used to quickly redispatch the 118-bus system when the projected path of the wildfire is expected to impact the region identified by the first row of Table I. The generator reschedule is shown in Fig. 2. In the figure, a positive (blue) bar indicates increase in the generator’s output, while a negative (red) bar indicates the opposite. The majority of generation shed occurs from the CMs identified in Table I. The FT algorithm and other security criteria ensure that this rescheduling does not increase vulnerability in other areas of the system (shown in subsequent results).

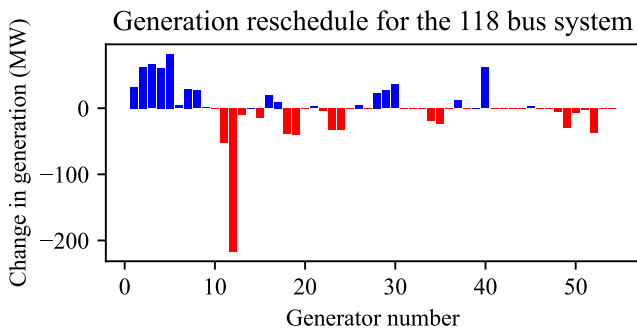
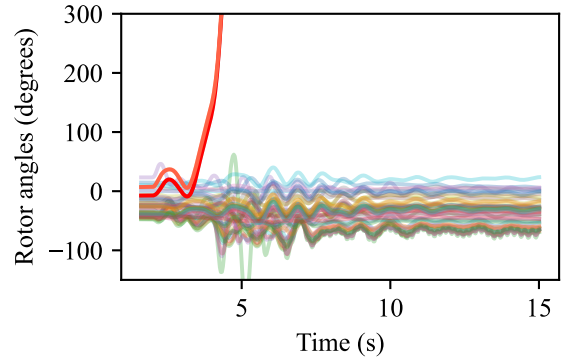
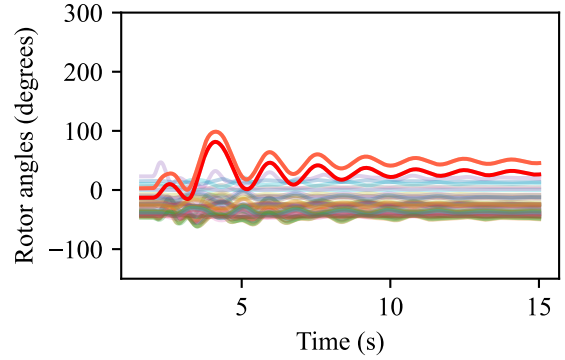


Fig. 2: CSCOPF redispatch schedule

A contingency analysis was done before and after implementation of the CSCOPF (Algorithm 1). Rotor angle trajectories for both cases are shown in Fig. 3. In the figure, the two CMs are highlighted in red and orange colors. Without any control, the CMs diverged and quickly lost synchronism. With CSCOPF, they remained synchronized with the rest of the system, effectively alleviating the transient instabilities.



(a) TDS without CSCOPF



(b) TDS with CSCOPF

Fig. 3: Rotor angle stability for the IEEE 118-bus system

Table III compares CSCOPF with a conventional real-time security constrained economic dispatch (RT-SCED), and a transient stability constrained OPF (TSCOPF). The RT-SCED does not have cut-set or stability constraints while the TSCOPF solution does not include cut-set constraints and performs SIME in real-time. During implementation, the RT-SCED did not reschedule sufficient generation for ensuring transient stability as it did not have any dynamic information (power from CMs was only lowered by 20 MW as compared to the minimum needed 118 MW shown in Table I). Moreover, in the identified cut-set, the power flow actually *increased* instead of decreasing, making that region of the network even more vulnerable to cascading line outages. In comparison, TSCOPF successfully alleviated the transient instabilities, but could not fully address the cut-set overloads (cut-set transfer only reduced by 57 MW as compared to the minimum needed 186 MW shown in Table I). This meant that the system was still at risk of cut-set saturation and line trips.

TABLE III: Comparative analysis of CSCOPF results

Result	RT-SCED	TSCOPF	CSCOPF
CM generation shed (MW)	20.4	118	269.79
Cut-set desaturation (MW)	-131.80	57.519	187.087
Total load shed (MW)	0	0	0
Transient stable	No	Yes	Yes
Cut-set secure	No	No	Yes
Time to solve (s)	0.066	0.256	0.066
Cost (\$/hr)	126,459.97	126,222.28	128,187.95

The proposed CSCOPF alleviated both static and dynamic vulnerabilities resulting in a resilient operation without incurring any load shed (see last column of Table III). The solution time of CSCOPF is similar to RT-SCED and one-fourth of TSCOPF, implying that the additional constraints do not increase the computational burden of the optimization. From an economic perspective, CSCOPF incurred an additional cost of \$1728/hr (over the RT-SCED solution). For context, in absence of any control, the simulated wildfire-induced contingency would have put about 534 MW of generation at risk of tripping (see Table I), which would have led to a loss in revenue of at least \$12,650/hr calculated on the generation side. Lastly, although load-shed was not required for the contingency-under-study, it is important to incorporate it in the problem formulation as a different contingency may require both generation redispatch as well as load-shed.

V. CONCLUSION

In this paper, a comprehensive corrective action scheme addressing both static and dynamic insecurities was introduced to ensure resilient power system operation during active wildfires. The scheme is based on an advanced contingency analysis tool that accurately analyses the impacts of such extreme event scenarios. The tool includes: (i) a static security component that is able to exhaustively desaturate cut-sets and prevent cascading line outages, thereby going beyond traditional security approaches that only protect against branch overloads, and (ii) a data-driven TSCP model that accurately and reliably predicts the appropriate correction factor for mitigating transient instabilities under varying loading conditions and prevents cascade tripping of generators. Finally, the LR-based implementation guarantees both transparency (in comparison to black-box models) as well as solution optimality.

The numerical results indicate that the proposed model is able to detect and alleviate cascading outage risks due to overloaded lines, generators, as well as cut-sets, while bearing minimal additional operational cost. Future work will analyse the ability of the proposed approach in mitigating the impacts of wildfires on renewable-rich systems from both stability as well as economic perspectives.

REFERENCES

- [1] K. Balaraman, "Wildfires pushed PG&E into bankruptcy. Should other utilities be worried?" *Utility Dive*, Nov. 19, 2020, <https://www.utilitydive.com/news/wildfires-pushed-pge-into-bankruptcy-should-other-utilities-be-worried/588435/>.
- [2] P. Moutis and U. Sriram, "PMU-driven non-preemptive disconnection of overhead lines at the approach or break-out of forest fires," *IEEE Transactions on Power Systems*, vol. 38, no. 1, pp. 168–176, 2023.
- [3] Y. Wu, Y. Xue, J. Lu, Y. Xie, T. Xu, W. Li, and C. Wu, "Space-time impact of forest fire on power grid fault probability," *Automation of Electric Power Systems*, vol. 40, no. 3, pp. 14–20, 2016.
- [4] D. A. Z. Vazquez, F. Qiu, N. Fan, and K. Sharp, "Wildfire mitigation plans in power systems: A literature review," *IEEE Transactions on Power Systems*, vol. 37, no. 5, pp. 3540–3551, 2022.
- [5] M. Choobineh, B. Ansari, and S. Mohagheghi, "Vulnerability assessment of the power grid against progressing wildfires," *Fire Safety Journal*, vol. 73, pp. 20–28, 2015.
- [6] NERC, "1,200 MW fault induced solar photovoltaic resource interruption disturbance report: Southern California 8/16/2016 event," <https://www.nerc.com/pa/rrm/ea/Pages/1200-MW-Fault-Induced-Solar-Photovoltaic-Resource-Interruption-Disturbance-Report.aspx>.
- [7] S. Dian, P. Cheng, Q. Ye, J. Wu, R. Luo, C. Wang, D. Hui, N. Zhou, D. Zou, Q. Yu, and X. Gong, "Integrating wildfires propagation prediction into early warning of electrical transmission line outages," *IEEE Access*, vol. 7, pp. 27 586–27 603, 2019.
- [8] H. Daochun, L. Peng, R. Jiangjun, Z. Yafei, and W. Tian, "Review on discharge mechanism and breakdown characteristics of transmission line gap under forest fire condition," *High Voltage Engineering*, vol. 41, no. 2, pp. 622–632, 2015.
- [9] C. Haseltine and L. Roald, "The effect of blocking automatic reclosing on wildfire risk and outage times," in *2020 52nd North American Power Symposium*, 2021, pp. 1–6.
- [10] J. J. Macwilliams, J. Kobus, and S. L. Monaca, "PG&E: Market and policy perspectives on the first climate change bankruptcy," 2019.
- [11] A. Shrestha and F. Gonzalez-Longatt, "Frequency stability issues and research opportunities in converter dominated power system," *Energies*, vol. 14, no. 14, 2021. [Online]. Available: <https://www.mdpi.com/1996-1073/14/14/4184>
- [12] R. S. Biswas, A. Pal, T. Werho, and V. Vittal, "A graph theoretic approach to power system vulnerability identification," *IEEE Transactions on Power Systems*, vol. 36, no. 2, pp. 923–935, 2020.
- [13] R. S. Biswas, A. Pal, T. Werho, and V. Vittal, "Mitigation of saturated cut-sets during multiple outages to enhance power system security," *IEEE Transactions on Power Systems*, vol. 36, no. 6, pp. 5734–5745, 2021.
- [14] J. Ma, J. C. Cheng, F. Jiang, V. J. Gan, M. Wang, and C. Zhai, "Real-time detection of wildfire risk caused by powerline vegetation faults using advanced machine learning techniques," *Advanced Engineering Informatics*, vol. 44, p. 101070, 2020.
- [15] "FlamMap," US Forest Service, Rocky Mountain Research Station, Fire, Fuel, and Smoke Science Program, <https://www.firelab.org/project/flammap>, last accessed October 2023.
- [16] M. Abdelmalak and M. Benidris, "Enhancing power system operational resilience against wildfires," *IEEE Transactions on Industry Applications*, vol. 58, no. 2, pp. 1611–1621, 2022.
- [17] J. Lu, J. Guo, Z. Jian, and X. Xu, "Optimal allocation of fire extinguishing equipment for a power grid under widespread fire disasters," *IEEE Access*, vol. 6, pp. 6382–6389, 2018.
- [18] A. Arab, A. Khodaei, R. Eskandarpour, M. P. Thompson, and Y. Wei, "Three lines of defense for wildfire risk management in electric power grids: A review," *IEEE Access*, vol. 9, pp. 61 577–61 593, 2021.
- [19] R. Bayani and S. D. Manshadi, "Resilient expansion planning of electricity grid under prolonged wildfire risk," *IEEE Transactions on Smart Grid*, vol. 14, no. 5, pp. 3719–3731, 2023.
- [20] S. Sahoo, A. I. Sifat, and A. Pal, "Data-driven flow and injection estimation in PMU-unobservable transmission systems," in *2023 IEEE Power & Energy Society General Meeting*. IEEE, 2023, pp. 1–5.
- [21] C. Guo, C. Ye, Y. Ding, and P. Wang, "A multi-state model for transmission system resilience enhancement against short-circuit faults caused by extreme weather events," *IEEE Transactions on Power Delivery*, vol. 36, no. 4, pp. 2374–2385, 2021.
- [22] Y. Zhang, L. Wehenkel, and M. Pavella, "SIME: A comprehensive approach to fast transient stability assessment," *IEEE Transactions on Power and Energy*, vol. 118, no. 2, pp. 127–132, 1998.
- [23] Y. Xu, J. Ma, Z. Y. Dong, and D. J. Hill, "Robust transient stability-constrained optimal power flow with uncertain dynamic loads," *IEEE Transactions on Smart Grid*, vol. 8, no. 4, pp. 1911–1921, 2017.
- [24] Siemens Industry Software Inc., *PSS[®]E*, Siemens, Washington, DC, 2023, version 35.0.0. [Online]. Available: <https://www.siemens.com/global/en/products/energy/grid-software/planning/pss-software/pss-e.html>
- [25] L. Gurobi Optimization, *Gurobi Optimizer Reference Manual*, Gurobi Optimization, LLC, 2023, version 10.0. [Online]. Available: <https://www.gurobi.com>
- [26] L. Thurner, A. Scheidler, F. Schäfer, J.-H. Menke, J. Dollichon, F. Meier, S. Meinecke, and M. Braun, "Pandapower," 2022, version 2.9.0. [Online]. Available: <http://www.pandapower.org>
- [27] A. B. Birchfield, T. Xu, K. M. Gegner, K. S. Shetye, and T. J. Overbye, "Grid structural characteristics as validation criteria for synthetic networks," *IEEE Transactions on Power Systems*, vol. 32, no. 4, pp. 3258–3265, 2017.